Samarium monoxide epitaxial thin film as a possible heavy-fermion compound

Yutaka Uchida, Kenichi Kaminaga, Tomoteru Fukumura, and Tetsuya Hasegawa

Phys. Rev. B **95**, 125111 — Published 8 March 2017

DOI: 10.1103/PhysRevB.95.125111

Samarium Monoxide Epitaxial Thin Film as a Possible Heavy Fermion Compound

Yutaka Uchida,[1,2] Kenichi Kaminaga,[1,2] Tomoteru Fukumura,[2,3,4*] and Tetsuya Hasegawa[1]

[1]Department of Chemistry, The University of Tokyo, Tokyo 113-0033, Japan

[2]Department of Chemistry, Tohoku University, Sendai 980-8578, Japan

[3]WPI-Advanced Institute for Materials Research, Tohoku University, Sendai 980-8577, Japan

[4]Center for Spintronics Research Network, Tohoku University, Sendai 980-8577, Japan

SmO (001) epitaxial thin films were grown on $YAlO_3$ (110) substrates by pulsed laser deposition method. X-ray photoemission spectroscopy indicated coexistence of Sm^{2+} and Sm^{3+}, suggesting a valence fluctuating state. SmO thin film showed metallic conduction like SmO polycrystal in previous study. However, SmO thin film showed nonmonotonical temperature dependence at low temperature in contrast with the polycrystal. A local resistivity minimum was observed at 16 K, probably caused by the dense Kondo effect, and the resistivity below 2 K was proportional to T^2. These features suggest heavy fermionic nature of SmO.

INTRODUCTION

Several rare earth compounds involving Ce, Yb, Pr, and Sm are heavy fermion compounds possessing unique properties such as the Kondo insulating state [1] and unconventional superconductivity [2,3], and are recently proposed as topological insulator, e.g. SmB_6 [4]. Rock-salt structure samarium monochalcogenides, SmS, SmSe, and SmTe, showed insulating to metal transition with the application of high pressure [5]. The insulator to metal transition was interpreted as a change in band structure due to the lattice shrinkage. The shrinkage induced the lowering of 5*d* conduction band minimum with respect to $4f^6$ level, resulting in electronic configuration of Sm ions to be $4f^6 \rightarrow 4f^5 + 5d$, in which 5*d* electrons are delocalized. This state corresponds to valence fluctuating state of Sm ion between Sm^{2+} and Sm^{3+}, in which the valence of each Sm ions is not fixed but varied spatially and temporally [6,7]. Hence, SmS is "black phase" semiconductor with fixed valence of Sm^{2+} under ambient pressure, and turns into "golden phase" metal with valence fluctuation between Sm^{2+} and Sm^{3+} under high pressure [5]. The average valence of Sm ions in the golden phase SmS was reported to be about +2.8 at 2.9 GPa [8]. The metallic SmS behaves as a heavy fermion compound, exhibiting large specific heat coefficient and T^2-linear resistivity at low temperature [9,10].

Alternative method for the insulator to metal transition is to decrease anion size of samarium monochalcogenides owing to the systematic decrease in bandgap with decreasing anion size. From SmTe to SmO, 5*d* conduction band minimum is lowered, thus SmO is expected to be heavy fermion metallic system even at ambient pressure like golden phase SmS (Fig. 1) [7,11,12]. So far, SmO has been only available in polycrystalline form with high pressure synthesis [11–13], and metallic conduction was observed [11]. In order to further investigate intrinsic properties of SmO, we evaluated the valence of Sm ion and measured the electrical transport property down to 0.5 K for SmO epitaxial thin film on lattice matched substrate for the first time.

EXPERIMENTAL SECTION

SmO epitaxial thin films were grown on $YAlO_3$ (110) substrates (a = 0.518 nm, b = 0.531 nm, c = 0.735 nm) by pulsed laser deposition method using KrF excimer laser (λ = 248 nm). The lattice mismatch was −5.2% along SmO [110] || $YAlO_3$ [001]. A commercial Sm metal (99.9%) pellet was used for a target. Prior to growth, $YAlO_3$ substrates were pre-annealed in a furnace at 1000 °C for 5 hours in order to obtain an atomically flat surface. For thin film growth, Sm seed layer was firstly grown on $YAlO_3$ (110) substrate at 400 °C in vacuum ($\leq 5.0 \times 10^{-8}$ Torr) for 50 minutes at a pulse repetition rate of 1 Hz. Subsequently, SmO film was grown on the seed layer at 400 °C in Ar and O_2 mixed gas (Ar : O = 99 : 1, 5.0×10^{-8} Torr in total) for 90 minutes at a pulse repetition rate of 10 Hz. In order to prevent the film from oxidization, AlO_x capping layer was in-situ grown in vacuum at room temperature after thin film growth. Typical thickness of SmO film was 70 nm. Crystal structure of SmO thin films was identified by X-ray diffraction (XRD) measurements (Bruker Discover with GADDS). For a reference, cubic Sm_2O_3 (001) epitaxial thin film with 28 nm thick was also grown on $SrTiO_3$ (001) substrate [14]. The valence of Sm in SmO and Sm_2O_3 was evaluated by X-ray photoemission spectroscopy (XPS), in which C 1*s* peak at 284.8 eV was used as a reference. Electrical resistivity was measured for 0.5−300 K at 0 T and for 2−300 K at 0−9 T using Hall-bar patterned films. The carrier was *n*-type and the carrier concentration was 7.4×10^{21} cm^{-3} at 300 K.

RESULTS AND DISCUSSION

Figure 2(a) shows out-of-plane θ-2θ XRD patterns of SmO thin films grown at 400 °C on $YAlO_3$ (110) substrates with and without seed layer [15]. Both films showed SmO 002 and 004 peaks indicating the formation of SmO (001) epitaxial thin films. The film without seed layer contained Sm_3Al phase whose properties have been unknown [16], while the film with seed layer was single phase with the full width at half maximum of the 002 rocking curve 2.25 °. The seed layer might protect interdiffusion of Al at the surface of $YAlO_3$. Figure 2(b) shows SmO 111 diffraction spot on asymmetric plane (χ = 35 °) measured with two dimensional detector. This result represents the epitaxial

relationship of SmO (001) on $YAlO_3$ (110) and SmO [110] || $YAlO_3$ [001]. The crystal structure was uniaxially distorted rock-salt structure with lattice constants of a = 0.496 nm and c = 0.502 nm. The larger lattice constants than that of cubic SmO (a = 0.494 nm) [11,12] was probably due to the presence of oxygen vacancies and/or the effect of tensile strain from substrates.

Figures 3(a) and (b) show XPS Sm $3d_{5/2}$ spectra of Sm_2O_3 and SmO thin film, respectively. The spectrum of SmO was deconvoluted into two spectra of Sm^{3+} and Sm^{2+}, whose maximum peaks are at 1081.4 eV and 1074.2 eV, respectively [17]. The former and the latter peaks showed good coincidence with those of Sm_2O_3 (Fig. 3(a)) and semiconducting SmS [18], respectively. The spectrum of SmO was similar to that of metallic SmS [18], indicating a valence fluctuating state between Sm^{2+} and Sm^{3+} in SmO. The average valence of the Sm ion in SmO was +2.9 calculated from the XPS areal peak intensity ratio, consistent with that of SmO polycrystal evaluated from its lattice constant, X-ray adsorption spectrum, and magnetic susceptibility [12]. From the XPS depth profile, Al content in the film was below detection limit. Thus, the influence of Sm_3Al phase on electric properties described below was negligible.

Figure 4(a) shows temperature dependence of resistivity for SmO thin film. From 30 K to 300 K, the resistivity showed almost T-linear dependence. With decreasing temperature, the resistivity decreased with local minimum at 16 K, then increased down to 10 K, and again decreased as shown in Fig. 4(b). These features were reproducible for different samples. This local resistivity minimum, that is rather indistinct due to the large residual resistivity, could be attributed to the dense Kondo effect owing to an interaction between Sm^{3+} ions and conduction electrons as seen in $SmTM_2Al_{20}$ (TM = Ti, V, Cr) [19], although such behavior has not been observed in SmO polycrystal [11]. From 0.5 K to 2 K, the resistivity was proportional to T^2 with T^2-coefficient A of 0.06 μΩcm/K^2 as shown in the inset of Fig. 4(b) [20]. This T^2-law is a characteristic of heavy fermion compounds [21], in which heavy fermion-like quasiparticle is formed by the coupling of conduction electrons and localized f electrons. The obtained A

value was as large as those of well-known heavy fermion compounds, e.g. ~0.08 μΩcm/K^2 for UPt [22,23].

It is noted that the dense Kondo effect was preserved even at 9 T with small negative magnetoresistance (Fig. 4(a)). Such magnetic field insensitive Kondo effect was attributed to valence fluctuation of Sm ions in several Sm-based ternary compounds [19,24–26], and the negative magnetoresistance was also observed [26]. The small lattice constants of SmO might contribute to the emergence of seemingly heavy fermionic state even without high pressure in contrast with the other Sm monochalcogenides [27]. The simple binary SmO with rock-salt structure in contrast with existing heavy fermion compounds would enable us to explore novel functionalities by designing e.g. heteroepitaxial structure. Indeed, a recent theoretical study proposed that SmO is a topological semi-metal possibly exhibiting the quantum anomalous Hall effect in an interface between EuO [28].

CONCLUSIONS

We obtained SmO epitaxial thin films and studied its electrical transport property. A valence fluctuating state was observed at ambient pressure in contrast with SmX (X = S, Se, Te). Different from the SmO polycrystal in previous studies, both the dense Kondo effect and T^2-law below 0.5 K were observed in the ρ-T curve, indicating that SmO is a heavy fermion compound. This compound with the rather simple rock-salt structure will be useful not only for improving our understanding on heavy fermion compounds but also for exploration of novel functionality by tailoring heteroepitaxial structure.

ACKNOWLEDGEMNT

Resistivity measurement was in part performed using facilities of the Cryogenic Research Center, The University of Tokyo. XPS measurement was conducted in Research Hub for Advanced Nano Characterization, The University of Tokyo, under the support of Nanotechnology Platform by MEXT, Japan (No. 12024046). This work is supported by JST-CREST and JSPS-KAKENHI (No. 26105002).

References

[1] P. S. Riseborough, Adv. Phys. **49**, 257 (2000).

[2] F. Steglich, J. Aarts, C. D. Bredl, W. Lieke, D. Meschede, W. Franz, and H. Schäfer, Phys. Rev. Lett. **43**, 1892 (1979).

[3] K. Hasselbach, L. Taillefer, and J. Flouquet, Phys. Rev. Lett. **63**, 93 (1989).

[4] M. Dzero, K. Sun, V. Galitski, and P. Coleman, Phys. Rev. Lett. **104**, 106408 (2010).

[5] A. Jayaraman, V. Narayanamurti, E. Bucher, and R. G. Maines, Phys. Rev. Lett. **25**, 1430 (1970).

[6] A. Chatterjee and A. K. Singh, Phys. Rev. B **6**, 2285 (1972).

[7] B. Batlogg, E. Kaldis, A. Schlegel, and P. Wachter, Phys. Rev. B **14**, 5503 (1976).

[8] P. P. Deen, D. Braithwaite, N. Kernavanois, L. Paolasini, S. Raymond, A. Barla, G. Lapertot, and J. P. Sanchez, Phys. Rev. B **71**, 245118 (2005).

[9] F. Lapierre, M. Ribault, F. Holtzberg, and J. Flouquet, Solid State Commun. **40**, 347 (1981).

[10] Y. Haga, J. Derr, A. Barla, B. Salce, G. Lapertot, I. Sheikin, K. Matsubayashi, N. K. Sato, and J. Flouquet, Phys. Rev. B **70**, 220406 (2004).

[11] J. M. Leger, P. Aimonino, J. Loriers, P. Dordor, and B. Coqblin, Phys. Lett. **80A**, 325 (1980).

[12] G. Krill, M. F. Ravet, J. P. Kappler, and L. Abadli, Solid State Commun. **33**, 351 (1980).

[13] J. M. Leger, N. Yacoubi, and J. Loriers, J. Solid State Chem. **36**, 261 (1981).

[14] H. Yang, H. Wang, H. M. Luo, D. M. Feldmann, P. C. Dowden, R. F. DePaula, and Q. X. Jia, Appl. Phys. Lett. **92**, 062905 (2008).

[15] The growth at 350 °C and at 450 and 500 °C resulted in the formation of Sm_3Al phase and the worse crystallinity, respectively.

[16] K. H. L. Buschow and J. H. N. van Vucht, Philips Res. Rep. **22**, 233 (1967).

[17] The XPS spectral shape was reproducible in different samples and almost unchanged during sputtering film surface, representing homogeneously distributed coexistence of Sm^{3+} and Sm^{2+} states.

[18] Y. Mori and S. Tanemura, Appl. Surf. Sci. **253**, 3856 (2007).

[19] A. Sakai and S. Nakatsuji, Phys. Rev. B **84**, 201106 (2011).

[20] A slight change in resistivity at 2 K between Fig. 4(b) and its inset was possibly due to the surface oxidation/degradation of SmO thin film.

[21] N. Takeda and M. Ishikawa, J. Phys. Condens. Matter **15**, L229 (2003).

[22] K. Kadowaki and S. B. Woods, Solid State Commun. **58**, 507 (1986).

[23] N. Tsujii, H. Kontani, and K. Yoshimura, Phys. Rev. Lett. **94**, 057201 (2005).

[24] A. Yamada, R. Higashinaka, R. Miyazaki, K. Fushiya, T. D. Matsuda, Y. Aoki, W. Fujita, H. Harima, and H. Sato, J. Phys. Soc. Jpn. **82**, 123710 (2013).

[25] R. Higashinaka, T. Maruyama, A. Nakama, R. Miyazaki, Y. Aoki, and H. Sato, J. Phys. Soc. Jpn. **80**, 093703 (2011).

[26] S. Sanada, Y. Aoki, H. Aoki, A. Tsuchiya, D. Kikuchi, H. Sugawara, and H. Sato, J. Phys. Soc. Jpn. **74**, 246 (2005).

[27] O. B. Tsiok, L. G. Khvostantsev, A. V. Golubkov, I. A. Smirnov, and V. V. Brazhkin, Phys. Rev. B **90**, 165141 (2014).

[28] D. Kasinathan, K. Koepernik, L. H. Tjeng, and M. W. Haverkort, Phys. Rev. B **91**, 195127 (2015).

Figure captions

FIG. 1. Schematic energy band diagrams of samarium chalcogenides under ambient pressure, modified from Ref. 7.

FIG. 2. (a) Out-of-plane θ-2θ XRD patterns of SmO thin films on $YAlO_3$ substrates with (red) and without (black) seed layer. Inset shows a magnified view. (b) Two-dimensional XRD pattern of asymmetric plane ($\chi = 45$ °) for SmO thin film. (c) A schematic crystal structure of SmO (001) thin film epitaxially grown on the $YAlO_3$ (110) substrate.

FIG. 3. Sm $3d_{5/2}$ XPS spectrum for (a) Sm_2O_3 thin film and (b) SmO thin film (circle). The deconvoluted Sm^{3+} (red) and Sm^{2+} (blue) spectra and their sum (solid curve) are also shown.

FIG. 4. (a) Temperature dependence of electrical resistivity for SmO thin film from 2 to 300 K. (b) Enlarged view of (a) from 2 to 30 K. The inset shows the resistivity from 0.5 to 2 K. Solid line denotes $\rho \propto T^2$.

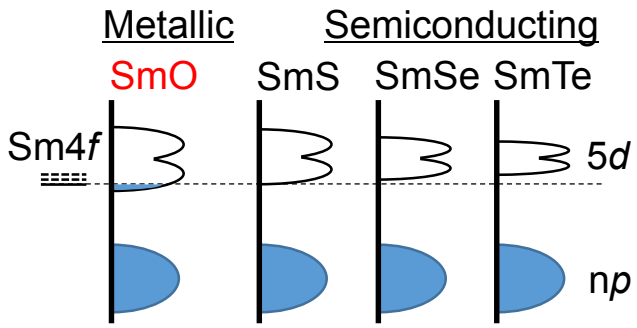

FIG. 1. Y. Uchida et al.

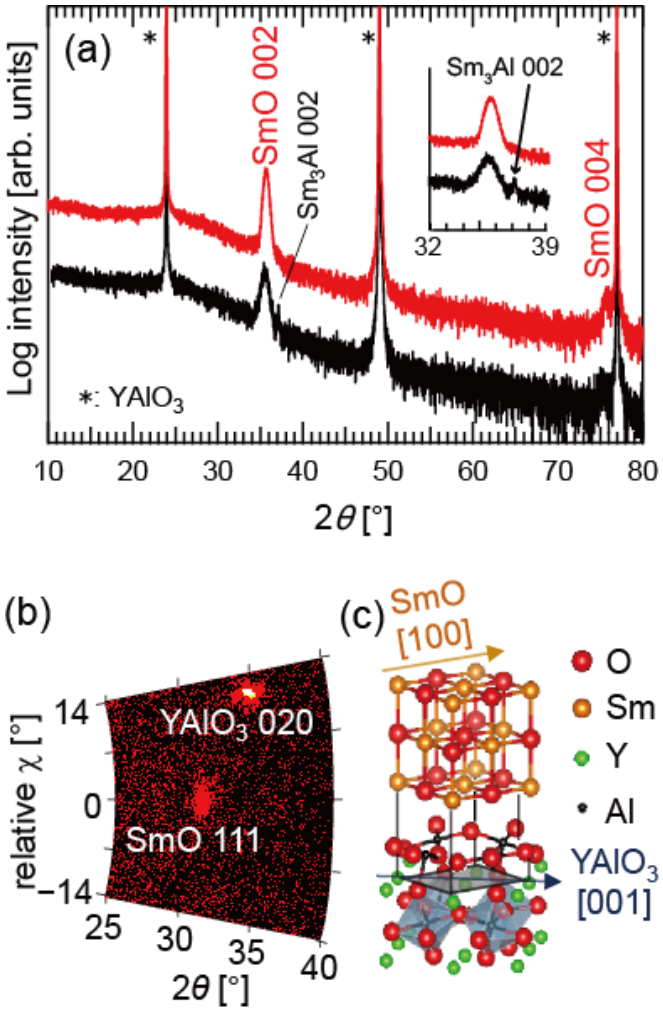

FIG. 2. Y. Uchida et al.

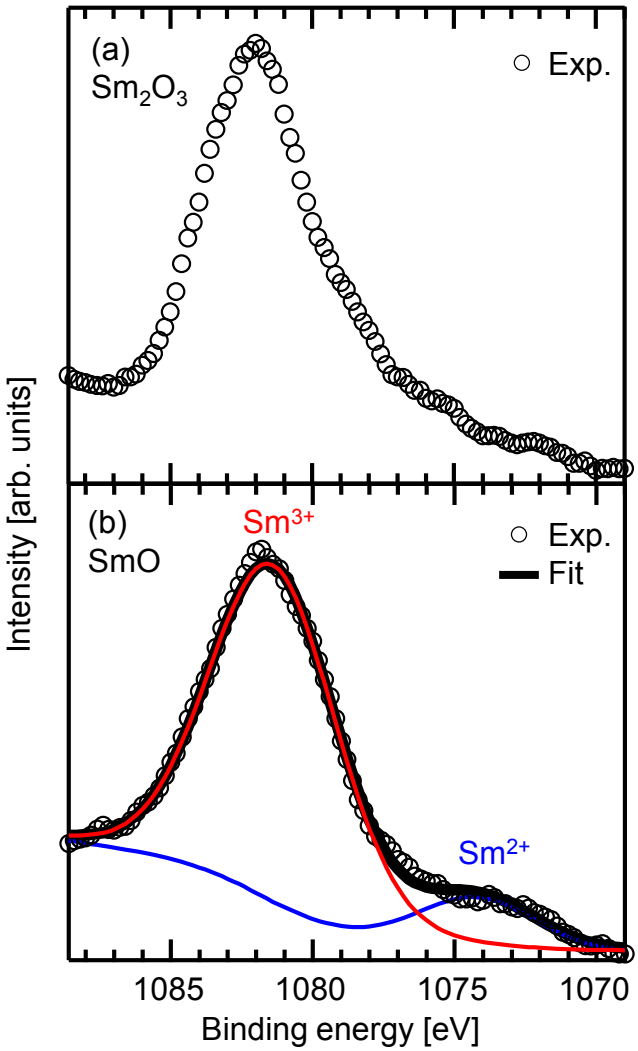

FIG. 3. Y. Uchida et al.

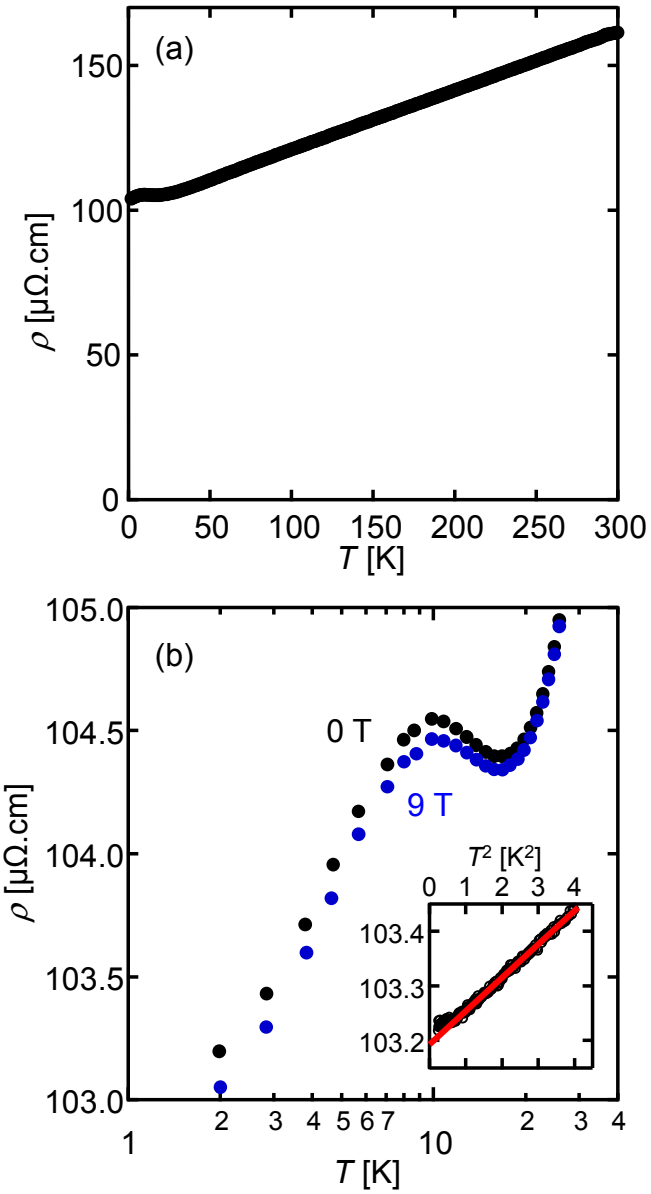

FIG. 4. Y. Uchida et al.